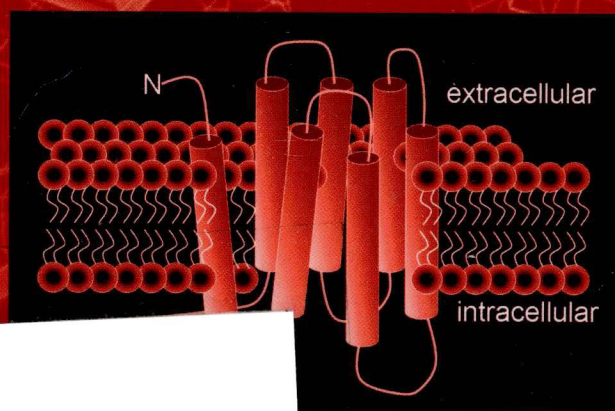


# Protein–Ligand Interactions

*Methods and Applications*

*Edited by*

G. Ulrich Nienhaus



METHODS IN MOLECULAR BIOLOGY™

# Protein–Ligand Interactions

*Methods and Applications*

Edited by

**G. Ulrich Nienhaus**

*Department of Biophysics, University of Ulm  
Ulm, Germany*

HUMANA PRESS  TOTOWA, NEW JERSEY

© 2005 Humana Press Inc.  
999 Riverview Drive, Suite 208  
Totowa, New Jersey 07512

[www.humanapress.com](http://www.humanapress.com)

All rights reserved. No part of this book may be reproduced, stored in a retrieval system, or transmitted in any form or by any means, electronic, mechanical, photocopying, microfilming, recording, or otherwise without written permission from the Publisher. Methods in Molecular Biology™ is a trademark of The Humana Press Inc.

All papers, comments, opinions, conclusions, or recommendations are those of the author(s), and do not necessarily reflect the views of the publisher.

This publication is printed on acid-free paper. ∞  
ANSI Z39.48-1984 (American Standards Institute) Permanence of Paper for Printed Library Materials.

Production Editor: Nicole E. Furia

Cover design by Patricia F. Cleary

Cover Illustration: (Foreground) Figure 1 from Chapter 18, "High-Throughput Screening of Interactions Between G Protein-Coupled Receptors and Ligands Using Confocal Optics Microscopy," by Lenka Zemanová, Andreas Schenk, Martin J. Valler, G. Ulrich Nienhaus, and Ralf Heilker; (Background) Figure 3B from Chapter 9, "Combined Use of XAFS and Crystallography for Studying Protein-Ligand Interactions in Metalloproteins," by Richard W. Strange and S. Samar Hasnain.

For additional copies, pricing for bulk purchases, and/or information about other Humana titles, contact Humana at the above address or at any of the following numbers: Tel.: 973-256-1699; Fax: 973-256-8341; E-mail: [orders@humanapr.com](mailto:orders@humanapr.com); or visit our Website: [www.humanapress.com](http://www.humanapress.com)

#### Photocopy Authorization Policy:

Authorization to photocopy items for internal or personal use, or the internal or personal use of specific clients, is granted by Humana Press Inc., provided that the base fee of US \$30.00 per copy is paid directly to the Copyright Clearance Center at 222 Rosewood Drive, Danvers, MA 01923. For those organizations that have been granted a photocopy license from the CCC, a separate system of payment has been arranged and is acceptable to Humana Press Inc. The fee code for users of the Transactional Reporting Service is: [1-58829-372-6/05 \$30.00].

Printed in the United States of America. 10 9 8 7 6 5 4 3 2 1

eISBN 1-59259-912-5

#### Library of Congress Cataloging in Publication Data

Protein-ligand interactions : methods and applications / edited by G. Ulrich Nienhaus.

p. ; cm. -- (Methods in molecular biology, ISSN 1064-3745 ; 305)

Includes bibliographical references and index.

ISBN 1-58829-372-6 (alk. paper)

1. Protein binding--Laboratory manuals. I. Nienhaus, G. Ulrich (Gerd Ulrich) II. Methods in molecular biology (Clifton, N.J.) ; 305.

[DNLN: 1. Ligands--Laboratory Manuals. 2. Proteins--chemistry--Laboratory Manuals.

3. Chemistry, Analytical--methods--Laboratory Manuals. 4. Protein Binding--Laboratory Manuals.

QU 25 P96665 2005]

QP551.P69599 2004

572'.6--dc22

2004042387

---

## Preface

The genomes of several organisms have been sequenced in recent years, and the efficient exploration of interactions among tens of thousands of gene products has moved to center stage in our quest for a detailed understanding of life at the molecular level. Molecular recognition and binding of ligands (atoms, ions, molecules) by proteins with high sensitivity and selectivity is of central importance to essentially all biomolecular processes. Therefore, a thorough understanding of protein–ligand interactions is of key importance for the basic and applied sciences. Techniques to study protein–ligand interactions have been established and refined for many years. They continue to be improved by the development of new reagents, protocols, and instrumentation. A variety of powerful experimental and theoretical tools have become available in recent years, and novel techniques are continually being introduced to meet new demands.

*Protein–Ligand Interactions: Methods and Applications* features a collection of methods for studying the interaction between proteins and ligands, including biochemical/bulk techniques, structure analysis, spectroscopy, single-molecule studies, and theoretical/computational tools. The present volume aims to provide the researcher with technical background information that will enable him or her to develop strategies for characterizing protein–ligand interactions in the most effective way. Life scientists in both academia and industry will find hands-on information regarding both established and novel approaches for the study of protein–ligand interactions. We have attempted to present a broad selection of widely applicable techniques. We hope that *Protein–Ligand Interactions: Methods and Applications* will provide a good starting point from which to embark on other, more specialized techniques.

I wish to thank all contributing authors for their hard work and considerable patience. I greatly appreciate the high quality of their presentations that made compiling this volume a particularly pleasurable experience.

**Gerd Ulrich Nienhaus**

---

## Contributors

- PHILIP A. ANFINRUD • *Laboratory of Chemical Physics, National Institute of Diabetes and Digestive and Kidney Diseases, National Institutes of Health, Bethesda, MD*
- ABEL BAERGA-ORTIZ • *Department of Chemistry and Biochemistry, University of California San Diego, La Jolla, CA*
- UTE CURTH • *Department of Biophysical Chemistry, Medizinische Hochschule, Hannover, Germany*
- ROBERT H. EIBL • *Department of Physiology and Biophysics, University of Miami School of Medicine, Miami, FL*
- ARNOLD M. FALICK • *Department of Chemistry and Biochemistry, University of California San Diego, La Jolla, CA*
- JOEL M. FRIEDMAN • *Department of Physiology and Biophysics, Albert Einstein College of Medicine, Bronx, NY*
- KLAUS GERWERT • *Department of Biophysics, Ruhr-University Bochum, Bochum, Germany*
- FRANK GESELLCHEN • *Department of Biochemistry, University of Kassel, Kassel, Germany*
- LUIS GRACIA • *Department of Physiology and Biophysics, Weill Medical College, Cornell University, New York, NY*
- HELMUT GRUBMÜLLER • *Theoretical and Computational Biophysics Department, Max-Planck-Institute for Biophysical Chemistry, Göttingen, Germany*
- MARK S. HARGROVE • *Department of Biochemistry, Biophysics and Molecular Biology, Iowa State University, Ames, IA*
- S. SAMAR HASNAIN • *Molecular Biophysics Group, College of Biology and Medicine, CCLRC Daresbury Laboratory, Daresbury, Warrington, Cheshire, UK*
- SERGIO A. HASSAN • *Center for Molecular Modeling, Division of Computational Bioscience, Center for Information Technology, National Institutes of Health, Bethesda, MD*
- THEODORE L. HAZLETT • *Laboratory for Fluorescence Dynamics, Department of Physics, University of Illinois at Urbana-Champaign, Urbana, IL*
- RALF HEILKER • *Department of Integrated Lead Discovery, Boehringer Ingelheim Pharma GmbH & Co KG, Biberach, Germany*
- FRIEDRICH W. HERBERG • *Department of Biochemistry, University of Kassel, Kassel, Germany*
- HYOTCHERL IHEE • *Department of Chemistry and School of Molecular Science, KAIST, Daejeon, South Korea*
- DAVID M. JAMESON • *Department of Cell and Molecular Biology, John A. Burns School of Medicine, University of Hawaii, Honolulu, HI*

- ANDREAS JANSHOFF • *Department of Physical Chemistry, Johannes-Gutenberg-University, Mainz, Germany*
- HERBERT P. JENNISSEN • *Department of Physiological Chemistry, University of Duisburg-Essen, Germany*
- ELIZABETH A. KOMIVES • *Department of Chemistry and Biochemistry, University of California San Diego, La Jolla, CA*
- CARSTEN KÖTTING • *Department of Biophysics, Ruhr-University Bochum, Bochum, Germany*
- EDWIN A. LEWIS • *Department of Chemistry and Biochemistry, Northern Arizona University, Flagstaff, AZ*
- MANHO LIM • *Department of Chemistry, Pusan National University, Busan, South Korea*
- H. PETER LU • *William R. Wiley Environmental Molecular Sciences Laboratory, Fundamental Science Division, Pacific Northwest National Laboratory, Richland, WA*
- JEFFREY G. MANDELL • *Department of Chemistry and Biochemistry, University of California San Diego, La Jolla, CA*
- RACHEL MARRINGTON • *Department of Chemistry, University of Warwick, Coventry, UK*
- TILL MAURER • *Department of Lead Discovery, Boehringer Ingelheim Pharma GmbH & Co KG, Biberach, Germany*
- GABOR MOCZ • *Biotechnology Program, Pacific Biomedical Research Center, University of Hawaii, Honolulu, HI*
- VINCENT T. MOY • *Department of Physiology and Biophysics, University of Miami School of Medicine, Miami, FL*
- KENNETH P. MURPHY • *Department of Biochemistry, University of Iowa, Iowa City, IA*
- G. ULRICH NIENHAUS • *Department of Biophysics, University of Ulm, Ulm, Germany*
- KARIN NIENHAUS • *Department of Biophysics, University of Ulm, Ulm, Germany*
- REINHARD PAHL • *Consortium for Advanced Radiation Sources, The University of Chicago, Chicago, IL*
- ALISON RODGER • *Department of Chemistry, University of Warwick, Coventry, UK*
- DAVID ROPER • *Department of Chemistry, University of Warwick, Coventry, UK*
- CARME ROVIRA • *Centre de Recerca en Química Teòrica, Parc Científic de Barcelona, Barcelona, Spain*
- QIAOQIAO RUAN • *Core R&D Biotechnology, Abbott Diagnostic Division, Abbott Laboratories, Abbott Park, IL*
- URI SAMUNI • *Department of Physiology and Biophysics, Albert Einstein College of Medicine, Bronx, NY*
- ANDREAS SCHENK • *Tecan Austria GmbH, Grödig, Austria*



- ILME SCHLICHTING • *Department of Biomolecular Mechanisms, Max Planck Institute for Medical Research, Heidelberg, Germany*
- MARIUS SCHMIDT • *Department of Physics, Technical University of Munich, Garching, Germany*
- VUKICA ŠRAJER • *Consortium for Advanced Radiation Sources and Department of Biochemistry and Molecular Biology, The University of Chicago, Chicago, IL*
- PETER J. STEINBACH • *Center for Molecular Modeling, Division of Computational Bioscience, Center for Information Technology, National Institutes of Health, Bethesda, MD*
- CLAUDIA STEINEM • *Institute of Analytical Chemistry, Chemo- & Biosensors, University of Regensburg, Regensburg, Germany*
- RICHARD W. STRANGE • *Molecular Biophysics Group, College of Biology and Medicine, CCLRC Daresbury Laboratory, Daresbury, Warrington, Cheshire, UK*
- SERGEY Y. TETIN • *Core R&D Biotechnology, Abbott Diagnostic Division, Abbott Laboratories, Abbott Park, IL*
- CLAUS URBANKE • *Department of Biophysical Chemistry, Medizinische Hochschule, Hannover, Germany*
- MARTIN J. VALLER • *Department of Integrated Lead Discovery, Boehringer Ingelheim Pharma GmbH & Co KG, Biberach, Germany*
- GEETHA VASUDEVAN • *Scientific Computing, Medarex Inc., Sunnyvale, CA*
- STUART WINDSOR • *Biotechnology Group, National Physical Laboratory, Teddington, Middlesex, UK*
- GREGOR WITTE • *Department of Biophysical Chemistry, Medizinische Hochschule, Hannover, Germany*
- LENKA ZEMANOVÁ • *Department of Biophysics, University of Ulm, Ulm, Germany*
- BASTIAN ZIMMERMANN • *Biaffin GmbH & Co KG, Kassel, Germany*

---

# Contents

Preface .....	v
Contributors .....	ix
1 Isothermal Titration Calorimetry <b>Edwin A. Lewis and Kenneth P. Murphy</b> .....	1
2 Direct Optical Detection of Protein–Ligand Interactions <b>Frank Gesellchen, Bastian Zimmermann, and Friedrich W. Herberg</b> .....	17
3 Label-Free Detection of Protein–Ligand Interactions by the Quartz Crystal Microbalance <b>Andreas Janshoff and Claudia Steinem</b> .....	47
4 Measurement of Solvent Accessibility at Protein–Protein Interfaces <b>Jeffrey G. Mandell, Abel Baerga-Ortiz, Arnold M. Falick, and Elizabeth A. Komives</b> .....	65
5 Hydrophobic Interaction Chromatography: <i>Harnessing Multivalent Protein–Surface Interactions for Purification Procedures</i> <b>Herbert P. Jennissen</b> .....	81
6 Sedimentation Velocity Method in the Analytical Ultracentrifuge for the Study of Protein–Protein Interactions <b>Claus Urbanke, Gregor Witte, and Ute Curth</b> .....	101
7 Protein–Ligand Interaction Probed by Time-Resolved Crystallography <b>Marius Schmidt, Hyotcherl Ihee, Reinhard Pahl, and Vukica Šrajer</b> .....	115
8 X-Ray Crystallography of Protein–Ligand Interactions <b>Ilme Schlichting</b> .....	155
9 Combined Use of XAFS and Crystallography for Studying Protein–Ligand Interactions in Metalloproteins <b>Richard W. Strange and S. Samar Hasnain</b> .....	167
10 NMR Studies of Protein–Ligand Interactions <b>Till Maurer</b> .....	197
11 Probing Heme Protein–Ligand Interactions by UV/Visible Absorption Spectroscopy <b>Karin Nienhaus and G. Ulrich Nienhaus</b> .....	215



12	Ultrafast Time-Resolved IR Studies of Protein–Ligand Interactions <b>Manho Lim and Philip A. Anfinrud</b> .....	243
13	Monitoring Protein–Ligand Interactions by Time-Resolved FTIR Difference Spectroscopy <b>Carsten Kötting and Klaus Gerwert</b> .....	261
14	Proteins in Motion: <i>Resonance Raman Spectroscopy as a Probe of Functional Intermediates</i> <b>Uri Samuni and Joel M. Friedman</b> .....	287
15	Fluorescence Polarization/Anisotropy Approaches to Study Protein–Ligand Interactions: <i>Effects of Errors and Uncertainties</i> <b>David M. Jameson and Gabor Mocz</b> .....	301
16	Ligand Binding With Stopped-Flow Rapid Mixing <b>Mark S. Hargrove</b> .....	323
17	Circular Dichroism Spectroscopy for the Study of Protein–Ligand Interactions <b>Alison Rodger, Rachel Marrington, David Roper, and Stuart Windsor</b> .....	343
18	High-Throughput Screening of Interactions Between G Protein- Coupled Receptors and Ligands Using Confocal Optics Microscopy <b>Lenka Zemanová, Andreas Schenk, Martin J. Valler, G. Ulrich Nienhaus, and Ralf Heilker</b> .....	365
19	Single-Molecule Study of Protein–Protein and Protein–DNA Interaction Dynamics <b>H. Peter Lu</b> .....	385
20	Application of Fluorescence Correlation Spectroscopy to Hapten–Antibody Binding <b>Theodore L. Hazlett, Qiaoqiao Ruan, and Sergey Y. Tetin</b> .....	415
21	Atomic Force Microscopy Measurements of Protein–Ligand Interactions on Living Cells <b>Robert H. Eibl and Vincent T. Moy</b> .....	439
22	Computer Simulation of Protein–Ligand Interactions: <i>Challenges and Applications</i> <b>Sergio A. Hassan, Luis Gracia, Geetha Vasudevan, and Peter J. Steinbach</b> .....	451
23	Force Probe Molecular Dynamics Simulations <b>Helmut Grubmüller</b> .....	493
24	Study of Ligand–Protein Interactions by Means of Density Functional Theory and First-Principles Molecular Dynamics <b>Carme Rovira</b> .....	517
	Index .....	555

## Isothermal Titration Calorimetry

Edwin A. Lewis and Kenneth P. Murphy

### Summary

Isothermal titration calorimetry is an ideal technique for measuring biological binding interactions. It does not rely on the presence of chromophores or fluorophores, nor does it require an enzymatic assay. Because the technique relies only on the detection of a heat effect upon binding, it can be used to measure the binding constant,  $K$ , the enthalpy of binding,  $\Delta H^\circ$  and the stoichiometry, or number of binding sites,  $n$ . This chapter describes instrumentation, experimental design, and the theoretical underpinnings necessary to run and analyze a calorimetric binding experiment.

**Key Words:** Binding; thermodynamics; proton linkage; enthalpy; heat capacity; data analysis.

### 1. Introduction

Titration calorimetry was first described as a method for the simultaneous determination of  $K$  and  $\Delta H$  about 40 yr ago by Christensen and Izatt (1,2). The method was originally applied to a variety of weak acid-base equilibria and to metal ion complexation reactions (3–5). These systems could be studied with the calorimetric instrumentation available at the time that was limited to the determination of  $K$  values less than about  $10^4$  to  $10^5 M^{-1}$  (6). The determination of larger association constants requires more dilute solutions and the calorimeters of that day were simply not sensitive enough.

Beaudette and Langerman published one of the first calorimetric binding studies of a biological system using a small volume TRONAC titration calorimeter (7). Their data for the titration of an enzyme, bovine liver glutamate dehydrogenase (GDH), with an inhibitor, adenosine diphosphate (ADP), are shown in Fig. 1. In 1979, Langerman and Biltonen published a description of microcalorimeters for biological chemistry, including a discussion of available

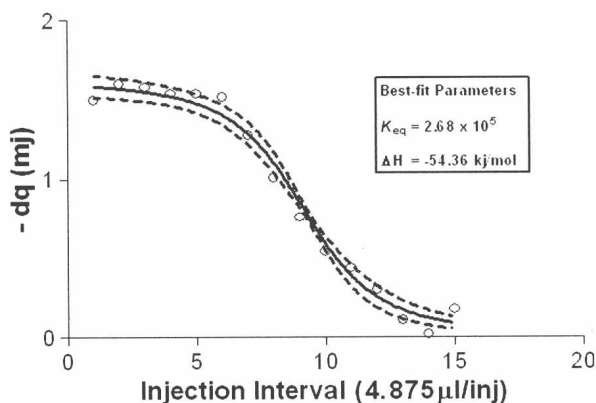


Fig. 1. Titration of 2.00 mL of 0.1340 M GDH with 6.17 mM ADP at pH 7.6 and 25°C. (Data taken from ref. 8.)

instrumentation, applications, experimental design, and data analysis and interpretation (8,9). This was really the beginning of the use of titration calorimetry to study biological equilibria. It took another 10 yr before the first commercially available titration calorimeter specifically designed for the study of biological systems became available from MicroCal (10).

Isothermal titration calorimetry (ITC) is now routinely used to directly characterize the thermodynamics of biopolymer binding interactions (11–13). This is largely a result of improvements in the ITC instrumentation and data analysis software. Modern instruments, like the MicroCal and Calorimetry Sciences Corporation ITCs, make it possible to measure heat effects as small as 0.4  $\mu\text{J}$  (0.1  $\mu\text{cal}$ ) allowing the determination of binding constants,  $K$ 's, as large as  $10^8$  to  $10^9 \text{ M}^{-1}$ .

In order to take full advantage of the powerful ITC technique, the user must be able to design the optimum experiment, understand the nonlinear fitting process, and appreciate the uncertainties in the fitting parameters  $K$ ,  $\Delta H$ , and  $n$ . ITC experiment design and data analysis have been the subject of numerous papers (14–17). This chapter reviews the planning of optimal ITC experiments, guides the reader through a sample experiment, the titration of RNase A with 2'-cytidine monophosphate (2'-CMP), and reviews theory underlying the nonlinear fitting of ITC data and the interpretation of ITC results.

## 2. Instrument Description

A schematic diagram of an isothermal titration calorimeter is shown in Fig. 2. The essential components of the ITC instrument are: (a) a matched pair of sample and reference cells contained within a thermostatted environment,

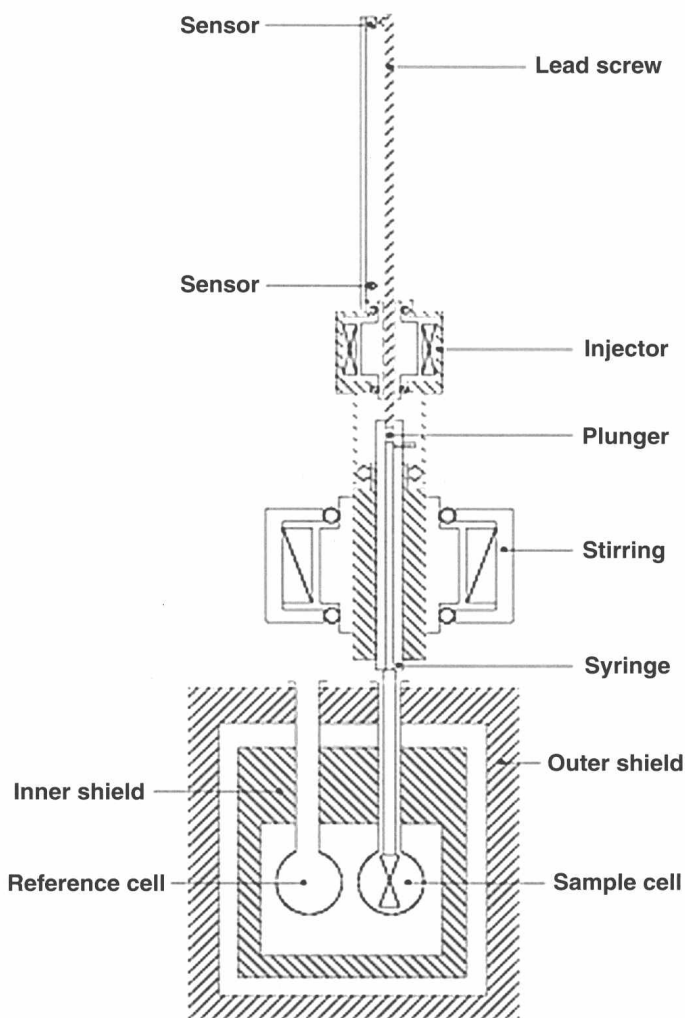


Fig. 2. Diagram of the MicroCal VP-ITC measuring unit (taken from the MicroCal website, <http://www.microcalorimetry.com/>).

(b) a stepper-motor-driven syringe for injecting titrant (ligand solution) into the sample cell, (c) a stirrer for keeping the contents of the sample cell homogeneous, and (d) a means for compensating (and measuring) the heat flow to the sample cell so that it is maintained at the same temperature as the reference cell. In modern ITC instruments, the cell volumes are nominally 1.5 mL, the temperature of the thermostat can be set from about 5 to 80°C, the injected volume can range from about 1 to 20  $\mu\text{L}$ , and heats as small as 0.4  $\mu\text{J}$  (0.1  $\mu\text{cal}$ ) can be measured.

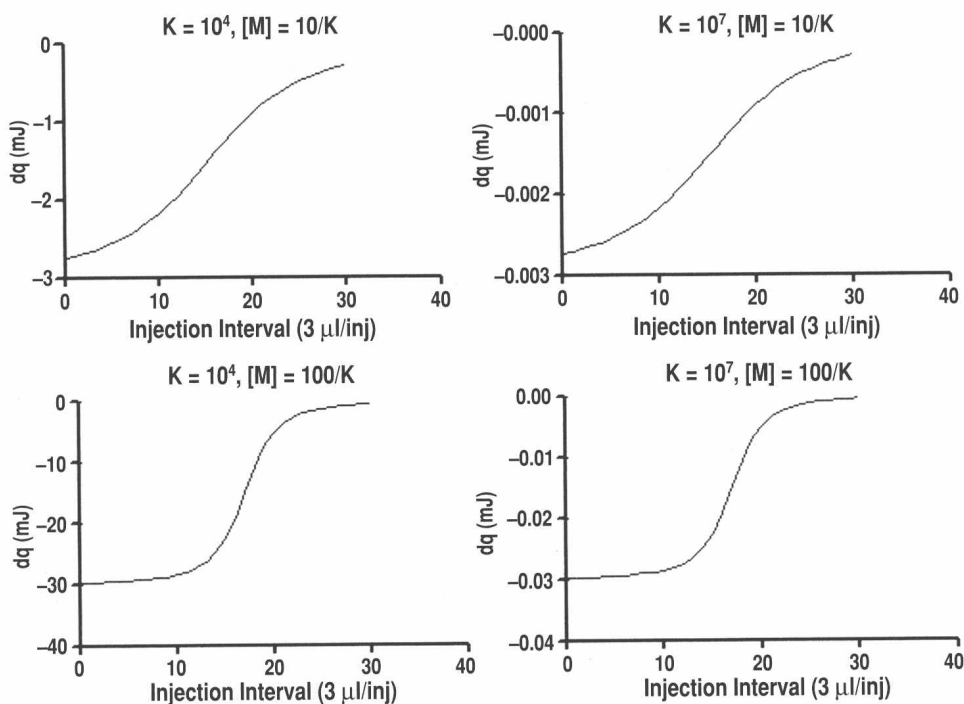


Fig. 3. Relationship between thermogram curvature and the  $c$  parameter,  $([M] \times K)$ , for two different values of  $c$ , 10 and 100.

The ITC signal is dependent on the concentrations of the macromolecule,  $[M]$ , and the ligand,  $[L]$ ; the cell volume; the injected volume; and the values of  $K$ ,  $\Delta H$ , and  $n$  (or a larger set of parameters for binding models more complicated than the  $n$  independent sites model). In order to obtain an estimate for  $K$ , the ITC experiment must yield a curved thermogram. Furthermore, of course, the ITC experiment must also be done under conditions that produce detectable amounts of heat for each titrant addition. These points are illustrated graphically in **Fig. 3**. The upper panels in **Fig. 3** show the curvature that would be observed in two experiments for systems with different binding constants,  $10^4$  and  $10^7 \text{ M}^{-1}$ , if the concentration of the macromolecule was chosen to be  $(10/K)$ , i.e.,  $[M] = 1 \text{ mM}$  for data shown in the upper left panel, and  $[M] = 1 \text{ } \mu\text{M}$  for the data shown in the upper right panel. The lower two panels in **Fig. 3** show thermograms for the same two systems with the exception that the macromolecule concentration was increased to be  $(100/K)$ . The first point that can be made from the data in **Fig. 3** is that the curvature is the same as long as the product of macromolecule concentration and  $K$  is held constant. It has been

widely reported that the  $c$  parameter,  $([M] \times K)$ , must be between 1 and 1000 in order to produce a thermogram with the curvature required for the simultaneous determination of  $K$  and  $\Delta H$  (10). The authors of this chapter believe that the best experiments will be done with the  $c$  parameter having a value between 10 and 100.

At first glance, each of the simulated thermograms in **Fig. 3** would seem to be representative of an experiment in which  $K$  and  $\Delta H$  could be accurately determined. On closer inspection, it is apparent that two of the experiments shown are less than optimal. The experiment shown in the upper right panel would yield heats that are too small to be determined accurately, even for the first injections where the largest heats would only be about 2.7 mJ (0.65 mcal), whereas the experiment shown in the lower left panel yields heats that are too large, approx 7000 mcal for the first injections, and the experiment would require excessive amounts of reagents. Clearly, simulations are important in optimizing the ITC experiment and in achieving a balance between detectable heats and curvature in the thermogram.

### 3. Methods

There are seven steps to running the ITC experiment. These are: 1) planning the experiment (simulations), 2) preparing the L and M solutions, 3) collecting the raw ITC data, 4) collecting the blank (L solution dilution), 5) correcting the raw ITC data, 6) nonlinear regression of the corrected titration data to provide estimates of the thermodynamic parameter values, and 7) interpretation of the model data. Each step will be discussed herein.

In our discussion of running the ITC experiment, we will use the binding of cytidine-2'-monophosphate, 2'-CMP, to bovine ribonuclease A, RNase, as a test system (10,18,19). These chemicals are available from Sigma Aldrich (St. Louis, MO) in suitable purity and have been widely used as a test system by ITC manufacturers. The approximate thermodynamic parameters for the 2'-CMP/RNase system are  $K \approx 6 \times 10^4 M^{-1}$  and  $\Delta H \approx -45$  kJ/mol with a stoichiometry of 1 at 25 °C (19). An alternative test system is the binding of  $Ba^{+2}$  ion by the cyclic poly ether, 18-crown-6 (19,20).

#### 3.1. Planning the Experiment

The first step in running the ITC experiment is to determine the concentrations for the macromolecule and ligand solutions. If the objective of the ITC experiment is only to determine the binding enthalpy change,  $\Delta H$ , then the only consideration is that the concentration of the ligand will be large enough that an accurately measurable heat effect,  $\geq 40$   $\mu J$  (10  $\mu cal$ ), will be observed and that the macromolecule concentration will be in excess. In the case of our test system, the binding of 2'-CMP to RNase, these conditions would be met



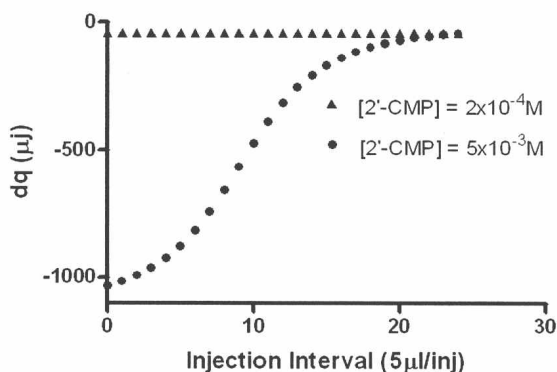


Fig. 4. Simulated experiments for the titration of a  $1.7 \times 10^{-4} M$  solution of RNase with two different titrant solutions. (2'-CMP at a concentration of either  $2 \times 10^{-4}$  or  $5 \times 10^{-3} M$ .)

with  $[2'\text{-CMP}] = 2 \times 10^{-4} M$ , and  $[\text{RNase}] = 1.7 \times 10^{-4} M$ . With an injection volume,  $v_{\text{inj}}$ , of  $5 \mu\text{L}$ , the heat per injection would be given by Eq. 1 below and there would be no curvature in the thermogram:

$$q_{\text{inj}} = \Delta H \times [L] \times v_{\text{inj}} = -45 \text{ kJ/mol} \times (2 \times 10^{-4}) M \times (5 \times 10^{-6}) \text{ l} \approx -45 \mu\text{J} (-11 \mu\text{cal}) \quad (1)$$

If the concentration of the L (2'-CMP) is increased to  $5 \times 10^{-3} M$ , the thermogram would show curvature similar to that shown in the lower panels of Fig. 3 ( $c = 10$ ) and an endpoint would be reached after approx 20 ( $5 \mu\text{L}$ ) injections. The integrated heat values for the first injections would now be more than  $-1000 \mu\text{J}$ . Increasing the concentration of RNase to  $1.7 \times 10^{-3} M$  ( $c = 100$ ) and the ligand concentration to  $5 \times 10^{-2} M$  would yield a thermogram showing the same curvature as that shown in the upper panels of Fig. 3. In this last case, the heat observed in the early injections would be too large, more than  $-10,000 \mu\text{J}$ . Fig. 4 shows simulated ITC data for experiments done under the first set of conditions where only  $\Delta H$  would be determined and under the second set of set of conditions where both  $K$  and  $\Delta H$  would be determined.

### 3.2. Solution Preparation and Handling

The final results of the ITC experiment depend on exact knowledge of the titrate and titrant solution concentrations, so it is imperative that the concentrations be determined as accurately as possible. Perhaps the ITC solutions can be made by volumetric dilution of stock solutions that were made up by weight. Whenever possible the concentrations should be verified by another analytical procedure (e.g., absorbance, kinetic activity, other analysis, etc.). As will be

noted later, it is especially important that the L concentration be known precisely, as errors in this value will affect the determination of both  $K$  and  $\Delta H$ .

It also is extremely important that the two solutions be matched with regard to composition, e.g., pH, buffer, salt concentration, etc. If the two solutions are not perfectly matched, there may be heat of mixing (or dilution) signals that overwhelm the heat signals for the binding reaction. It is typical that the solution of the macromolecule is dialyzed against a large volume of the buffer. The artifact heats of mixing can be minimized by using the dialysate from preparation of the macromolecule solution as the *solvent* for preparation of the ligand solution.

### 3.3. Correcting the Raw ITC Data

Obviously, the dialysis/dialysate approach will virtually eliminate the mixing or dilution effects for all solute species in common between the macromolecule and ligand solutions. The exception is that the heat of dilution for the ligand itself must be measured in a blank experiment. In this blank experiment, the ligand solution is titrated into buffer in the sample cell. The heat of dilution of the macromolecule should also be measured in a second blank experiment. This is done by simply injecting buffer from the syringe into the macromolecule solution in the sample cell. Usually the heat of dilution of the macromolecule measured in this way is negligible. To be completely rigorous, a third blank experiment should also be done. This buffer into buffer experiment may be thought of as an instrument blank. The equation to correct the heat data for dilution effects is:

$$Q_{\text{corr}} = Q_{\text{meas}} - Q_{\text{dil, macromolecule}} + Q_{\text{instrument blank}} \quad (2)$$

The blank corrections are for the same injection volumes as used in the collection of the actual titration data. In the case of the 2'-CMP/RNase titration experiment shown in **Fig. 5**, the only significant correction is for the dilution of the titrant (the results of the 2'-CMP dilution blank experiment are also shown in **Fig. 5**).

Another complicating reaction encountered in many biological binding experiments results from the release (or uptake) of protons as binding occurs. The released protons are taken up by the buffer conjugate base, and there are contributions to the heat both from binding protons to buffer and from the heat of removing protons from the macromolecule (17). The treatment of this complicating reaction requires knowledge of the number of protons released (or taken up) and the heat of ionization of the buffer. The measured enthalpy is given by:

$$\Delta H_{\text{meas}} = \Delta H_0 - \Delta H_{\text{ion}} \times n_p \quad (3)$$

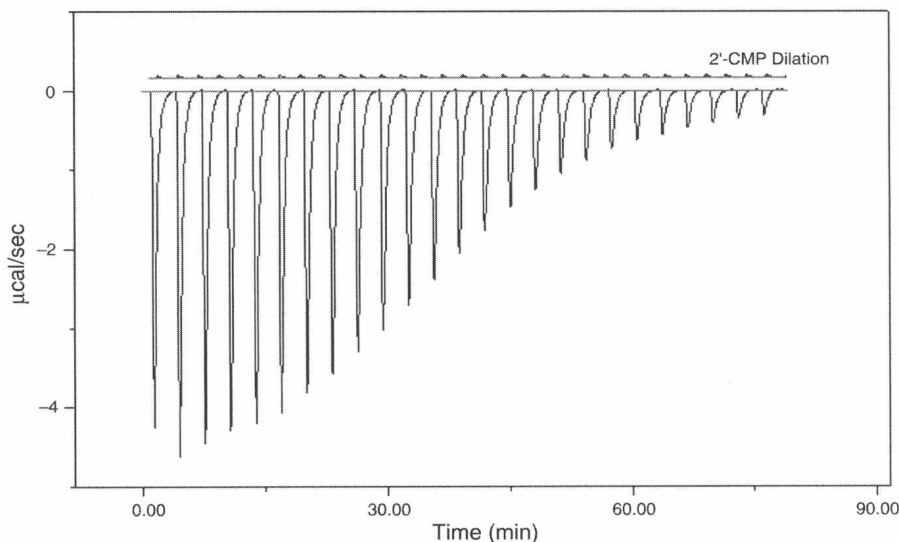


Fig. 5. The raw ITC data (power vs time) are shown for two titrations. The larger heat pulses are from the titration of 1.4 mL of a  $1.55 \times 10^{-4} M$  RNase solution with a  $3.19 \times 10^{-3} M$  solution of 2'-CMP. The smaller heat pulses are for the dilution of 5 mL of the 2'-CMP titrant into 1.4 mL of the acetate buffer. The power is given in units of mcal/s (where  $1 \text{ mcal/s} = 4.184 \text{ mJ/s} = 4.184 \text{ mW}$ ).

where  $\Delta H_0$  is the enthalpy of binding in the absence of a heat from protons binding to the buffer,  $\Delta H_{\text{ion}}$  is the heat of proton ionization for the buffer and  $n_p$  is the number of protons released on binding 1 mole of L. The value of  $n_p$  is determined from titrations done in at least two buffers with different heats of ionization. It should be emphasized that  $\Delta H_0$  includes the heat of protons being released from the protein upon binding and, as such, does not represent the *intrinsic* heat of the protein L interaction (17). Instead, it simply removes the contribution of the buffer. This phenomenon also provides an approach to manipulating the heat signal for a reaction that is accompanied by proton release. By simply using a buffer with a large heat of ionization, the heat signal can be enhanced. Alternatively, the use of a buffer with a small  $\Delta H_{\text{ion}}$  ( $\approx 0$ ) could be used to minimize the *artifact signal*.

Finally, because the generation of bubbles in the sample (or reference) solutions during an ITC experiment will generate spurious heat signals, the solutions should be degassed prior to filling the cell and injection syringe. The ITC manufacturers provide vacuum degassing accessories for this purpose. Precautions need to be taken to avoid boiling the solutions and changing the concentrations. Also, the ITC manufacturers supply cell loading syringes and